We are IntechOpen,
the world's leading publisher of
Open Access books
Built by scientists, for scientists

4,800
Open access books available

122,000
International authors and editors

135M
Downloads

Our authors are among the

154
Countries delivered to

TOP 1%
most cited scientists

12.2%
Contributors from top 500 universities

BOOK CITATION INDEX
CLARIVATE ANALYTICS
INDEXED

WEB OF SCIENCE™

Selection of our books indexed in the Book Citation Index
in Web of Science™ Core Collection (BKCI)

Interested in publishing with us?
Contact book.department@intechopen.com

Acoustics in Optical Fiber

Abhilash Mandloi and Vivekanand Mishra

Additional information is available at the end of the chapter

1. Introduction

Optical filters are the heart of optical networks; without the wavelength selective device wavelength division multiplexing and dense wavelength division multiplexing network will not exist. As the networks are progressing towards closer wavelength spacing, performance requirement for filters are becoming more demanding. Currently, the popular filters include gratings, thin-film filters, and Fabry-Perot filters and acoustoi optic tunable filters (AOTFs).

Acousto-optic (AO) effect in fibers has been studied to produce tunable filters, gain flatteners, modulators, frequency shifters, and optical switches reported. Most AO devices work on coupling from the fundamental mode (LP_{11}) of light to a higher order asymmetrical (LP_{ll}, LP_{12} .... LP_{1n}) modes. Acousto-optics is defined as the discipline devoted to the interactions between the acoustic waves and the light waves in a material medium. Acoustic (vibrational) waves can be made to modulate, deflect and focus light waves by causing a variation in the refractive index. Acousto optic tunable filters are a promising technology for dynamic gain equalization of optical fiber amplifiers [1]. By launching an acoustic wave directly on the fiber, the device combines the merits of fiber and AOTF devices namely the low insertion loss, low polarization dependence loss, wide tunability, fast tuning speed and ease of packaging. When a flexural acoustic wave is applied to a tapered single mode fiber, coupling takes place between the core mode and the cladding mode. The coupled energy in the cladding mode is essentially absorbed by the fiber jacket as reported so that the device is a notch filter. It means the centre frequency and the rejection efficiency can be tuned by adjustment of the frequency and voltage being applied. Varying the amplitudes and frequency of a RF generator can change the spectral profile of these filters.

To improve the rejection efficiency of the filters, the thickness of the fiber can be reduced. This is achieved through the heating and the acid-etching method. In the heating method, the ratio of cladding to core size is maintained while in the acid etching-method, the ratio between the cladding and core can be changed.

2. Acousto-optic tunable filter

2.1. Device design

The fiber used in our experiment is a Corning SMF-28, standard telecommunication single mode fiber. A region of SMF is etched by dipping the fiber in a hydrofluoric acid solution, which has a concentration of 40%. Etching rate controls the thickness of the SMF and the diameter reduction is observed using a CCD camera.

When the optical signal enters the fiber and interacts with the acoustic energy in a jacket stripped segment of the fiber, the core mode of the light is converted to a higher order cladding mode producing a notch filter like characteristics in the transmission spectrum. Core mode converting to various cladding modes will produce a few notch filters, with each having its peak notch at a separate wavelength [2-4]. A vibrating PZT transducer driven by a RF generator produces the acoustic energy as stated by Yun, Hwang and Kim, (1996). The acoustic energy is further amplified and concentrated to the fiber by a machined aluminium horn.
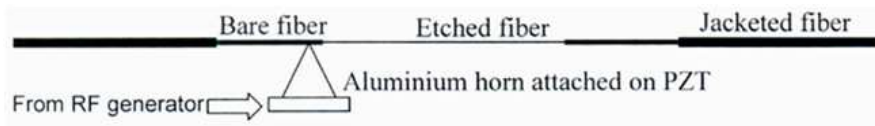

Figure 1. The setup to study AO interaction inside a fiber.

2.2. Horn design

An acoustic horn functions to transfer and amplify the surface acoustic wave to the fiber. All horns made were conical in shape, where the tip is narrow and the base is broad as described by Lee, Kim Hwang and Yun, (2003). All the horns fabricated for the AOTF experiment have a ratio of length to outer diameter ratio of 2. Length is defined as the length from the tip of the horn to the base of the horn. Horns taken are 1cm in length. Outer diameter of the horn is defined at the diameter at the base. The inside of the horns are made hollow. When the horn is made considerably small, the frequency dependence on the acoustic generator is low. In the experiments done, no transduction is observed when the fiber is not etched. Potential problems can be attributed to the size of the transducer and the adhesive used to bond the tip of the horn to the fiber. Solder acts as a strong, metallic, thermally stable, and acoustically transmitting joint. In these experiments however glue was chosen as the bonding agent. Of particular interest will be the horn tip size. Acoustic impedance at the horn tip is given by:

$$Z_r = c_a v_a A_r \tag{1}$$

where c_a is the longitudinal velocity inside aluminium, v_a is the density aluminium and A_r is the cross section of the horn tip. Acoustic impedance at the bond junction along the fiber is given by:

$$Z_s = 2c_s v_s A_s \tag{2}$$

where c_s is the longitudinal velocity inside silica, v_s is the density silica and A_s is the cross section of fiber. Acoustic impedance inside the fiber is counted twice because of bidirectional acoustic movement along the fiber. Optimum transduction occurs when $Z_r = Z_s$ and since acoustic impedance of silica is almost matching that of aluminium, according to engan et. al maximum acoustic wave transfer occurs when horn tip diameter is almost matching that of the fiber.

2.3. Tuning of peak wavelength

By driving a piezoelectric (PZT) device at an ultrasonic frequency the periodic perturbations can be created inside the fiber. In a phase-matched condition, where the momentum and energy conservation requirement $(L_B = \wedge)$ are met, the resonant frequency of an acoustic wave according to Birks, Russel and Culverhouse (1992) is given by

$$f = \frac{\pi b C_{ext}}{L_B^2} = \frac{\pi b C_{ext}}{\Lambda^2}$$

(3)

where b is the radius of the fiber, C_{ext} is the speed of fundamental acoustic mode, which for silica is 5760 ms⁻¹, $\wedge$ is the period of the microbend[1].

Assuming a phase-matched condition, the frequency needed to transfer the modes from core to cladding mode for various thickness of the fiber is given in Fig 2 and Fig 3. As the fiber diameter is reduced, the values of $df/d\lambda$ get smaller. For unetched fibres, the frequencies used to create the micro bends and thus, convert the modes are from 1.75 MHz to 2.25 MHz. For thin diameter fibers (20 μ m, 30 μ m, 40 μ m), the frequencies are from 800 kHz to 1.1 MHz.
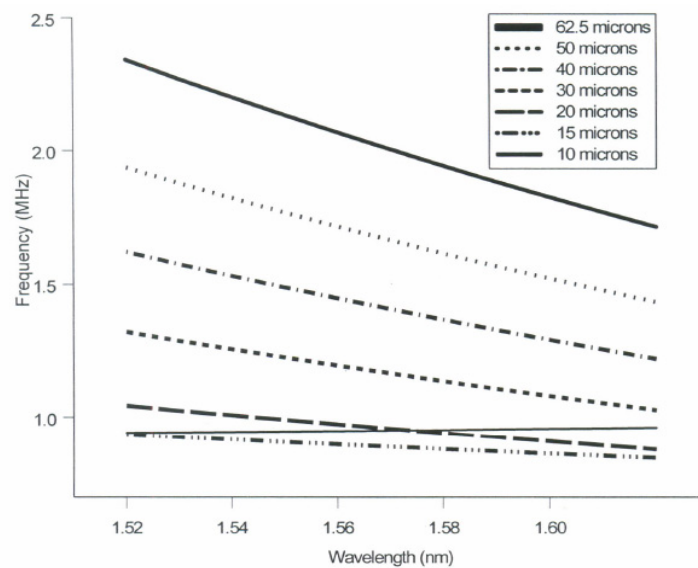

Figure 2. Calculated RF frequency to convert the LP01 mode to LP11 mode plotted against wavelength (for various thickness of fibre diameter).

---

[1] A microbend is the physical deformation of fiber achieved mechanically or chemically done to perturbing the optical modes to study mode coupling between core and cladding mode.
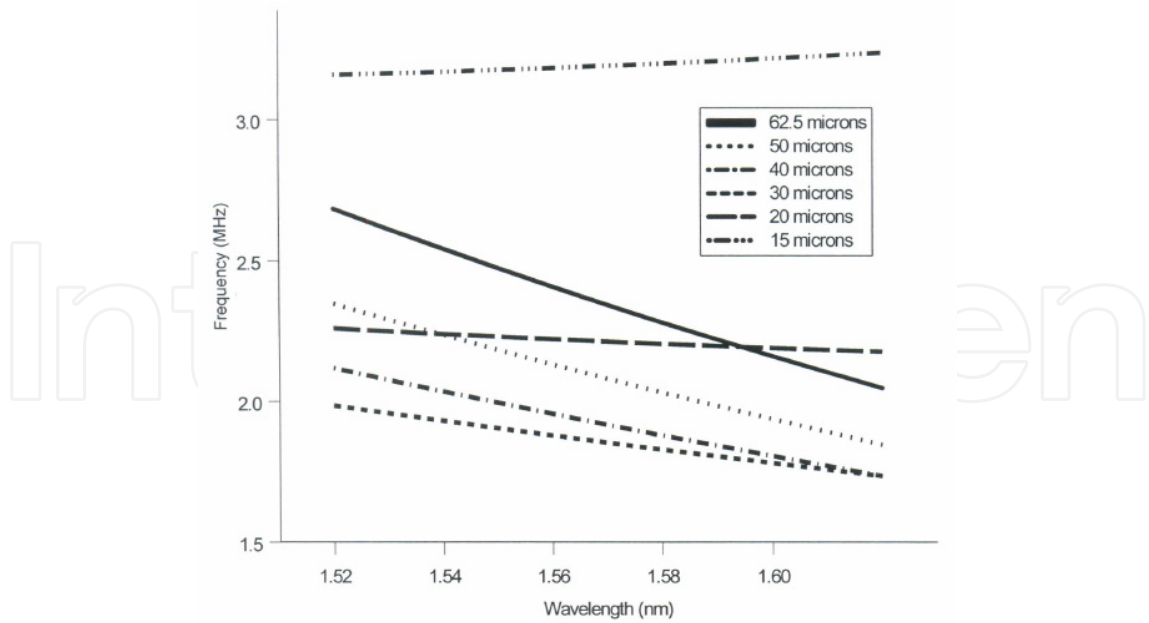
Figure 3. Calculated RF frequency to convert the LP0l mode to LP12 mode plotted against wavelength (for various thickness of fibre diameter).

Frequency from the RF generator can be used to control the peak wavelength tuning of the notch filters (Fig.4). The fiber used in the experiment has a diameter of 30 μm, and length of 17 cm. Higher frequencies of the RF generator will blue shift the peak wavelength of the filter [3-7]. The tuning range of the filter is slightly less than 300 nrn. From Eq.1.3, we deduce that, micro bend's period is inversely proportional to the frequency of the RF generator. For a larger value of period, the filter's peak is red shifted. Thin fibers have lower period values, thus etching the fibres will blue shift the peak wavelength of the notch filters. Frequency used to tune the peak wavelength as in for thin fibres is from 800 kHz to 1.1 MHz, which is in excellent agreement with the theory as in Fig.3 and Fig.4.
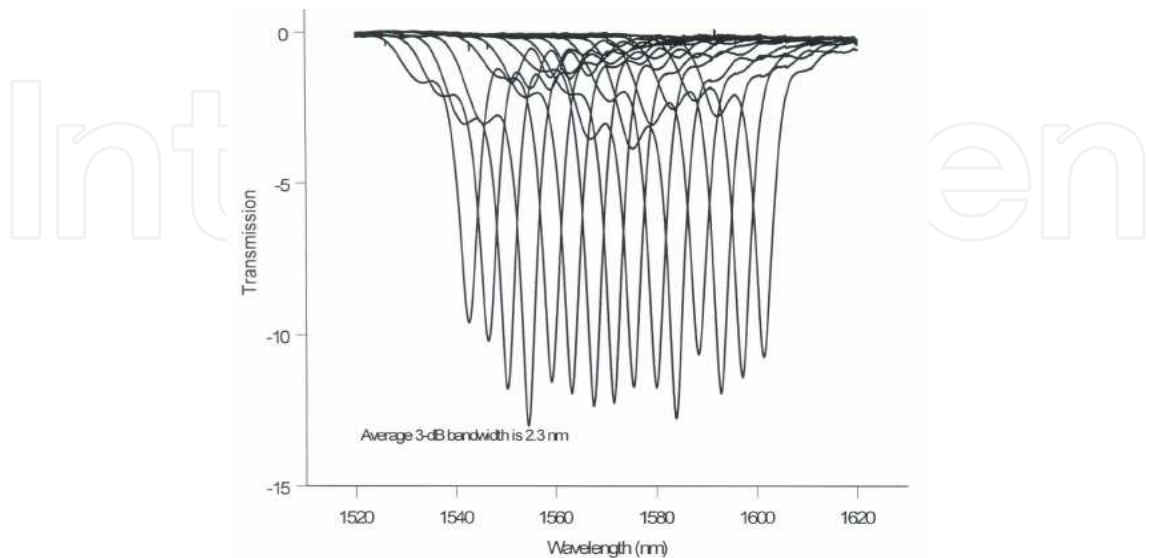

Figure 4. Measured peak wavelength tuning of the filter by changing the RF frequency. Frequency used is from 970 kHz to 1045 kHz. The fiber used has a thickness of 30 μm and length of 17 cm.

3. Tuning of attenuation depth

The RF generator's $V_{\text{p-p}}$ level will be used to control the attenuation depth of the filter. $V_{\text{p-p}}$ level is actually referring to the acoustic power transferred to the fiber. Increasing the $V_{\text{p-p}}$ level will generally increase the bottom level of the filter as seen from Fig. 5. However in some cases increasing the $V_{\text{p-p}}$ level will only distort the shape of the filter without increasing the notch's depth. For this strong over-coupled phenomenon, side lobes of the filter is actually increasing. One way to eliminate the problem is by limiting the interaction length of light inside the etched region. Here the power means RF generator's Vp-p level which will be used to control the attenuation depth of the filter [8-10]. Vp-p level is actually referring to the acoustic power transferred to the fiber. Increasing the Vp-p level will generally increase the bottom level of the filter as seen from Fig. 5. Here acoustic power supplied to PZT is 1.6 W to allow mode conversion.
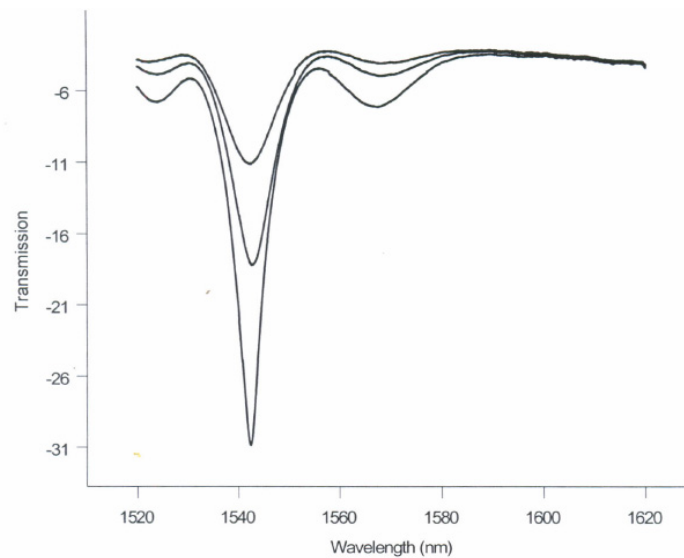

Figure 5. Measured attenuation variation of filter when the power of RF generator ($V_{\text{p-p}}$) is increased.

An effort to reduce the acoustic power fed into the fiber is by reducing the thickness of the fiber. The minimum acoustic power required by the device to operate or to allow mode conversion, is given by

$$P = 2\pi^3 \rho v_g (fR)^2 (u_t)^2 \tag{4}$$

where ρ is the mass density of the fiber (ρ =2200kg/m3 for fused silica), V_g is the group velocity of the wave and R is is curvature of fiber, and u_t is the transverse acoustic amplitude which is given by:

$$u_t = \frac{\pi}{2} L_B \frac{a}{L} \frac{1}{0.908} \tag{5}$$

where L is referring to the interaction length of acoustic and light inside the fiber and L_B is the optical beat length. Fig. 6 shows the calculated power required for mode conversion is

lower for etched fibers. When the fiber is unetched the power required will be 287 mW. For a 20 μ m fiber, the power required for conversion is only 1.17 mW.

Experimentally, as seen from Fig. 7 for a 37 μm thick fiber, the acoustic power supplied to PZT is 1.6 W to allow mode conversion. Mode conversion was confirmed using far-field radiation pattern as reported by Doma, and Blake (1992). However, in a *26 μ m* fiber, power requirement for mode conversion is reduced to a mere value of 42 mW. The difference in the power reduction with the calculated value, suggests that the loss at the point of contact is high[10]. It is believed that the horn design is still not optimized; nevertheless, this transduction is sufficient to demonstrate conversion between two modes. Typically, only the lowest order flexural acoustic mode should be made to travel inside the fiber, and this can be achieved by ensuring the horn tip's thickness is matching that of the fiber.
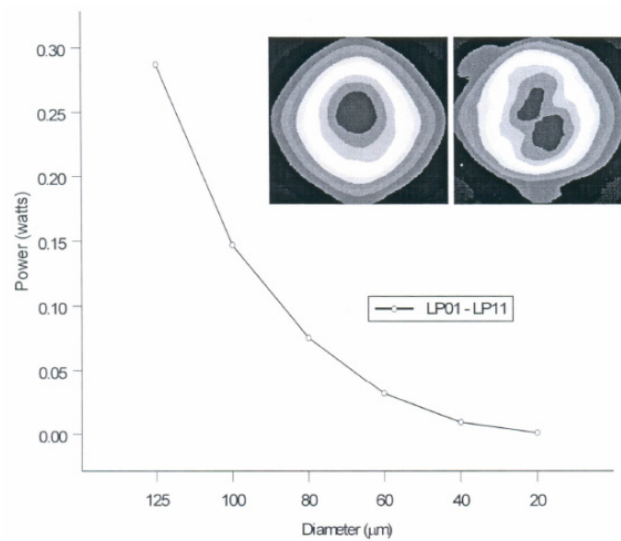

Figure 6. Calculated acoustic power required to allow mode conversion. Interaction length was set to 13 cm. Inset: Far field radiation pattern of modes involved in conversion. Left- LP01, Right- LP11.
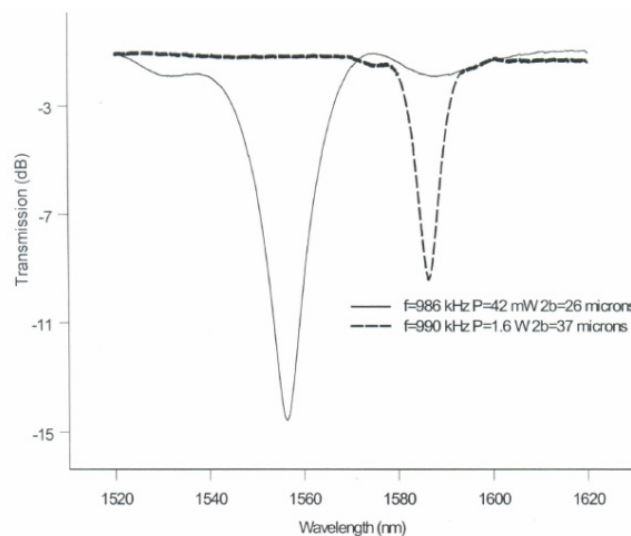

Figure 7. Measured transmission spectrum when fiber is etched. Significant reduction in acoustic power is observed.

4. Tuning of 3-dB bandwidth

The 3-dB bandwidth of the notch filter is given by the equation below as reported by D. Ostling, H.E. Engan (1995):

$$\Delta\lambda = \frac{0.8}{L}\left[\frac{\partial L_B(\lambda)}{\partial \lambda}\right]^{-1}\left[L_B(\lambda)\right]^2 \qquad (6)$$

Where λ is the wavelength of the light, L is the length of the coupling interaction, and L_B is the optical beat length [11-14]. For a broadband filter, a short coupling length, a long beat length and small beat length dispersion is required. Without making the device short, only by etching the fiber to that thickness a broad filter can be obtained as reported. However this bandwidth is not tuneable and so is not suitable for spectral shaping. In this section, a similar achievement by only using a SMF to tune the 3-dB bandwidth of the filter is demonstrated. In this device, the notch filter's attenuation, peak wavelength tuning and 3-dB bandwidth can be simultaneously controlled in a single device.

To achieve this, a tunable acoustic absorber is added to the original AO setup as shown in Fig. 8. By moving the acoustic absorber along the etched region of the fiber, the interaction of light inside the acoustic region can be controlled. From Eq.6, we know that by controlling the coupling interaction length the 3-dB bandwidth of the filter can be controlled [15]. A strong acoustic absorbing material such as cotton or polystyrene can be used as the acoustic absorber [16]. The absorbing material functions to ensure no surface acoustic wave beyond the absorber's position are present. Since the interaction length of light inside the acoustic region can be controlled, over-coupling phenomenon can be monitored, to reduce the effects of undesirable side lobes. Broad filters require higher power to operate when the attenuation level is maintained the same as a narrow filter.
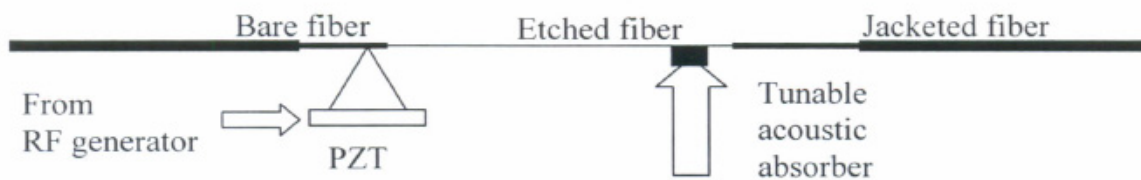
Figure 8. Setup to study the bandwidth variation using the AO interaction inside fiber.

From Fig. 9, the narrowest filter with a 3-dB bandwidth of 13 nm is obtained when maintaining the interaction length at 14 cm while the broadest filter with a 3-dB bandwidth of 28 nm is obtained when the interaction length is reduced to 7 cm. For an interaction length of 11.5 cm the spectral width is 16 nm and for 9 cm the spectral width will be 21 nm. The frequency used for wavelength tuning was from 960 kHz to 995 kHz and was sufficient to cover a wavelength span of 100 nm (1520 om-1620 nm).

For the broadest filter, the RF generator's V_{P-P} needed to generate coupling between the modes, seem to be the highest at 14 V. Meanwhile, for the narrowest filter, the V_{P-P} needed is only 6 V. Thus, we need a higher V_{P-P} to generate filters for shorter interaction length of light

inside the grating region [17]. The introduction of tuneable acoustic absorber will change the strain dependency on the device. To limit the strain change introduced in the device only the tip of the absorber is allowed to touch the fiber, in our case, the resonant frequency change corresponding to the strain change was maintained at +/- 0.7kHz. Throughout the experiment the total IL was maintained less than 0.1 dB and the PDL was less than 0.4 dB.
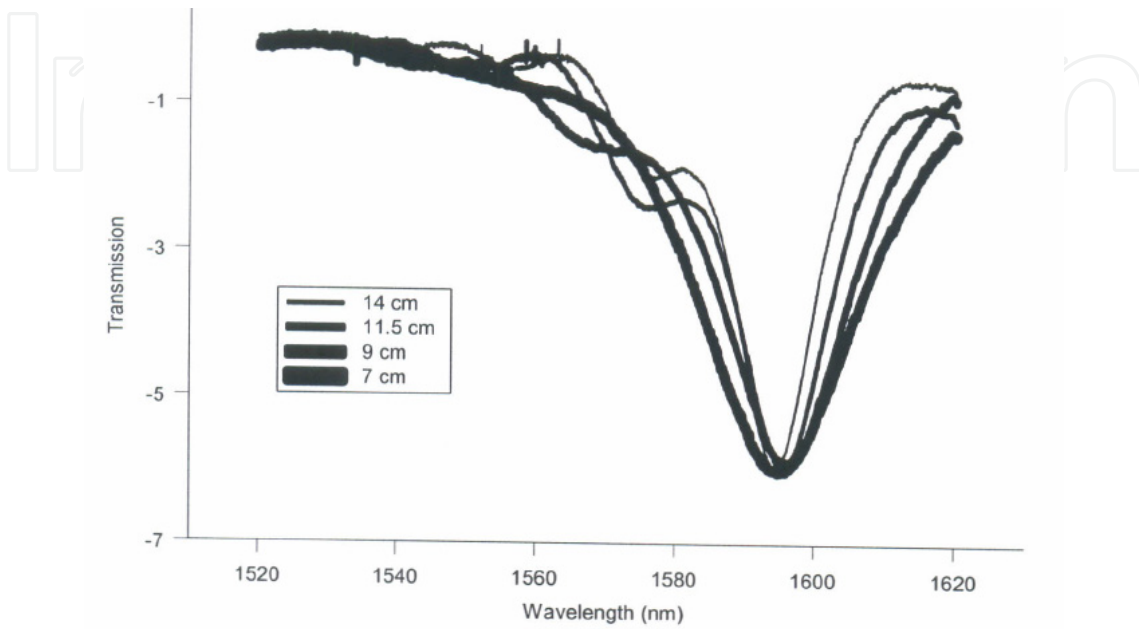
a)
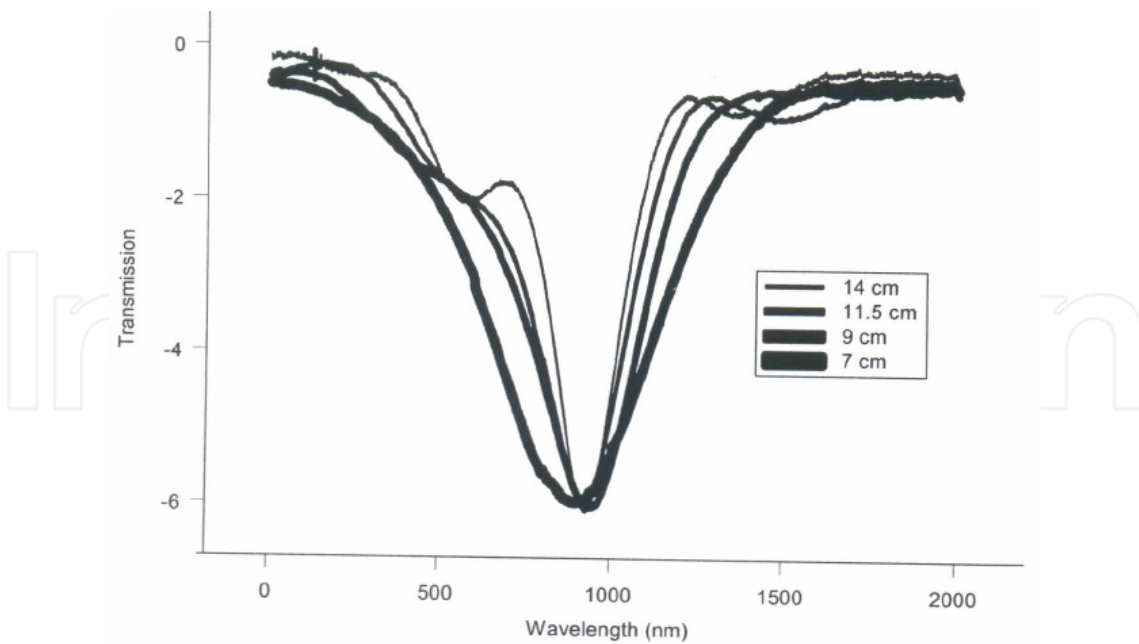
b)

a) 1596 nm b) 1566 nm

Figure 9. Measured bandwidth variation of filters at different peak wavelengths

5. Double-pass configuration

One of the key problems in fiber-based AOTF is the low attenuation level of the notch filter. Superposing two or more filters according to Yun, Lee, Kim and Kim (1999) produced by multiple transducers can increase the attenuation level. But this method introduces a very high crosstalk in the device especially when the filter's peak: wavelengths are very near to each another and prove [18] highly impractical. Alternatively to improve the attenuation level of the filter, a double pass AO setup reported by Satorious, Dimmick, Burdge (2002) and Culverhouse, Yun, Richardson, Birks, Farwell, Russell (1997) can be used. In the new setup as in Fig 1.10, a 3-port circulator is added before and after the AO device. Light comes in from port 1 of circulator 1 and goes through the acoustic region and experiences mode conversion. The LP 11 coupled mode is converted back to the fundamental mode at the jacket of the fiber. The light rounds circulator 2 and goes through the AO device and experiences mode conversion again. The produced notch filter is observed using the OSA connected to the port 3 of circulator 1. Since the period of the acoustic inside the fiber is not changed, the light going through this region experiences mode conversion at the same wavelength of the incident and returning light.

The insertion loss (IL) of a double-pass is increased to less than 3 dB and the Polarization Dependent Loss (PDL) was less than 0.6 dB. IL was not intentionally increased to a high value here, because 2 FC/FC connectors were introduced in the setup to connect port 2 of both circulators to the AO device. Splicing the ports to the device will reduce the IL loss to values less than 1 dB. Using higher quality circulators can further reduce PDL of the notch filters. The filters however will be more expensive to fabricate.
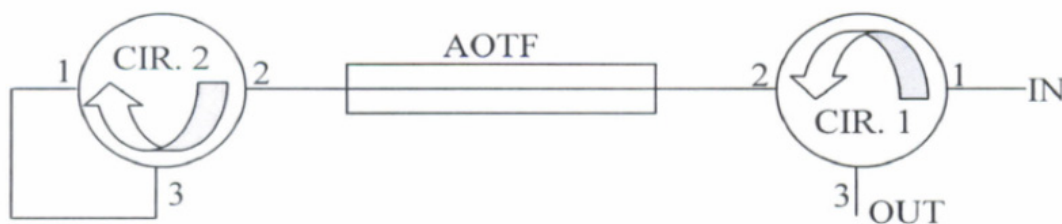

Figure 10. Double pass configuration to increase the maximum attenuation of the notch filter.

The AO band pass filter by Satorius *et. al.*, mentions side lobe suppression and maximum attenuation suppression using the double-pass configuration. Unlike the band pass filter, the notch filter will increase the side lobe level and maximum attenuation level using the double-pass configuration. The side lobe increment is not significant to exceed the bottom level of the main lobe of the notch filter.

From Fig. 11 the maximum attenuation of the notch filter was -28 dB for the double pass configuration and -12 dB for the single pass configuration. The maximum attenuation of the filter was increased to more than two times. The 3-dB bandwidth of the single pass AO device is 6.14 nm and the 3-dB bandwidth of the double pass AO device is 2.383 nm. This technique will be useful in producing narrow filters with high attenuation suitable in

switching applications. However, there will be a frequency shift of 7 nm introduced using this setup.

The optical signal coupled from the slow mode (LP01) to the fast mode (LP11) will be downshifted in frequency when the acoustic wave is in the same direction as the optical signal. Frequency is shifted up when the fast mode is coupled to the slow mode for the same acoustic wave [19]. The frequency shift direction is reversed when the acoustic wave is in opposite direction with the optical signal as reported by Kim, Blake, Engan, and Shaw, (1986). In a double-pass setup, the optical signal is both the same and opposite direction to the acoustic wave, while in a single-pass setup, optical signal is maintained in the same direction as the acoustic wave. Thus, a frequency shift is observed in a double-pass setup.
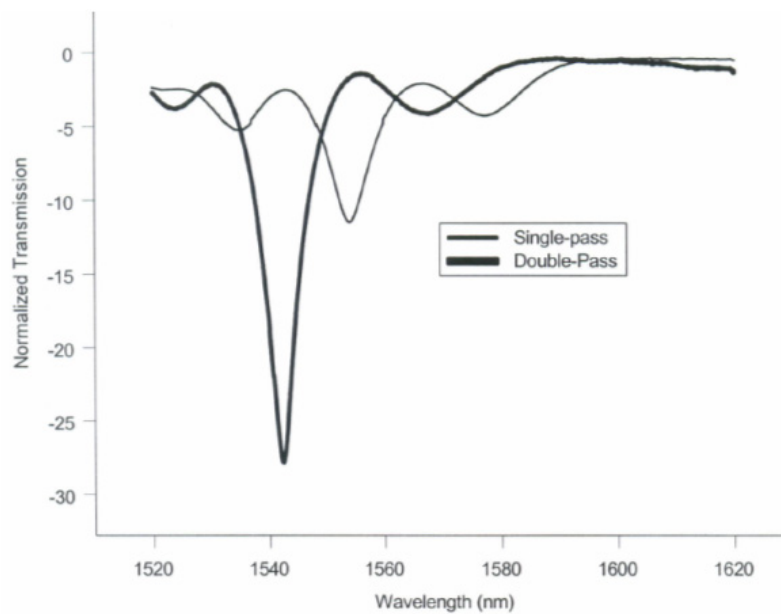

Figure 11. Measured normalized transmission spectrum using the double pass configuration. The result is compared with single pass configuration (refer to Fig4.1). There is a frequency shift of 7 nm to the left using the double-pass setup.

6. Gain flattening filter

The technique to vary the 3-dB bandwidth of filter inside SMF is then extended as a dynamic gain equalizer for the gain profile of an Erbidium Doped Fiber Amplifier (EDFA). This is just one of the possible applications of AO interaction as efficient spectral shaping devices. Various efforts to dynamically control the gain flatness of the ASE spectrum using acousto-optic tuneable filters (AOTF) were well demonstrated. Passive gain equalization as reported by Vengsarkar, Pedrazzani, Judkins, Lemaire, Bergano, and Davidson (1996) is unable to encounter gain variations due to different input optical power of Wavelength Division Multiplexing (WDM) channels. Meanwhile, integrated AOTF as gain flattening filters have a serious limitation of high insertion loss and crosstalk problems. Fiber-based AOTF by H.S. Kim, Park, and B.Y. Kim (1998) and the setup by Feced, Alegria, and Zervas

(1999) uses two transducers with six synthesizers to obtain the desired spectral filters. In this technique, to shape the gain, the AOTF setup is using only one transducer and a single-taper. This is possible because the 3-dB [21-24] bandwidth of the filter we demonstrated can be varied on the same device. In our setup to flatten the gain profile of the Amplified Stimulated Emission (ASE) spectrum, an AOTF device with two frequency generators and a double-branched power combiner is used as in Fig 12. The power combiner typically introduces a 3-dB loss to the system, thus higher Vp-p from the RF generator is needed to produce the filters for spectral shaping. Total insertion loss of the setup is less than 0.2 dB. For the measurement, the EDF A was used as the ASE source and the output spectrum measured [20] using an Optical Spectrum Analyser (OSA).
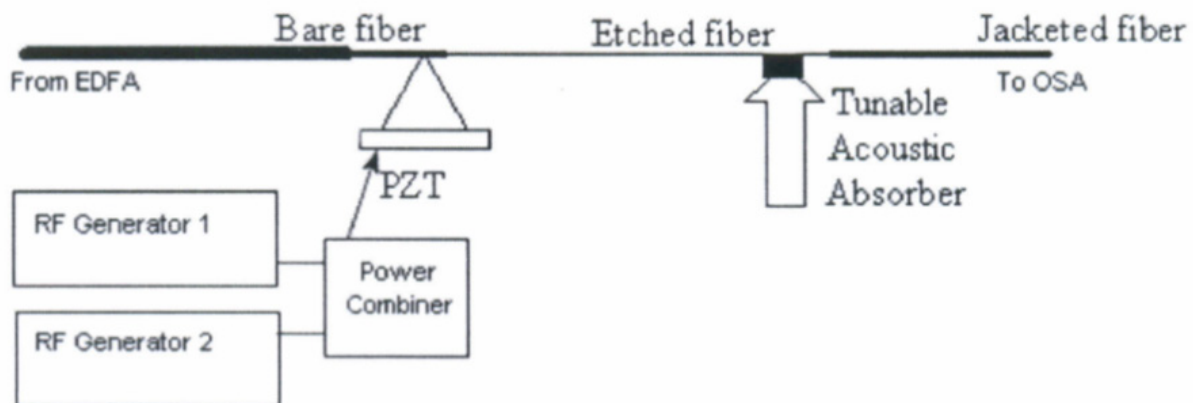

**Figure 12.** AOTF setup to flatten the gain of ASE spectrum.

The gain was flattened by changing the $V_{P\text{-}P}$ level of the RF generator, and moving the tuneable acoustic absorber along the etched region of the SMF. The degree of freedom to shape the filter is very high, thus the necessity of cascading another AOTF to the setup is not needed. Fig. 13 shows the effect of shaping the filter on the Amplified Stimulated Emission spectrum of EDFA. Typically has it Amplified Stimulated Emission s peaks at 1532 run and 1550 run. For low gain, however there is a single broad peak at 1560 run. By using this method we show that, the [26-28] ASE spectrum can be flattened regardless of the peak's position and bandwidth using the same device. Since the tuning range is about 300 run, any Amplified Stimulated Emission spectrum that is lying from 1350 run to 1630 run can be successfully flattened using the same device.
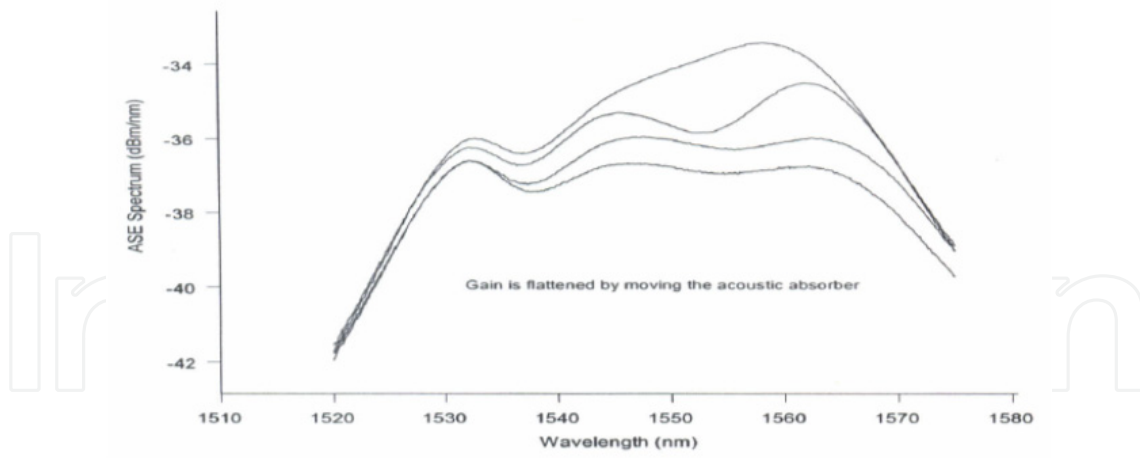
a)
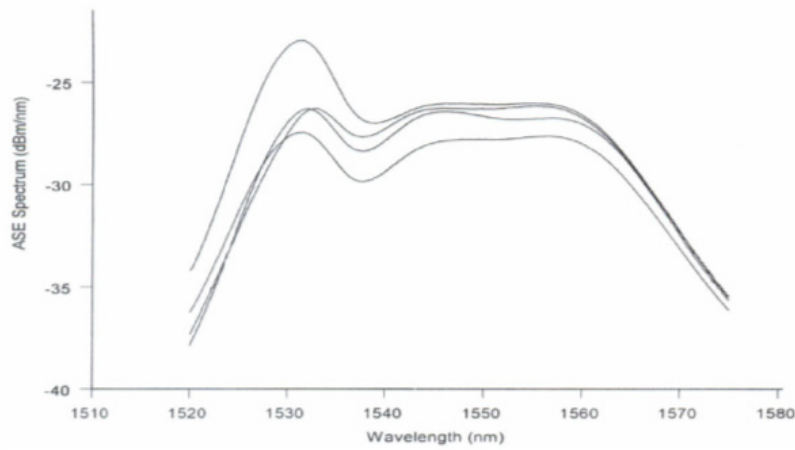
b)
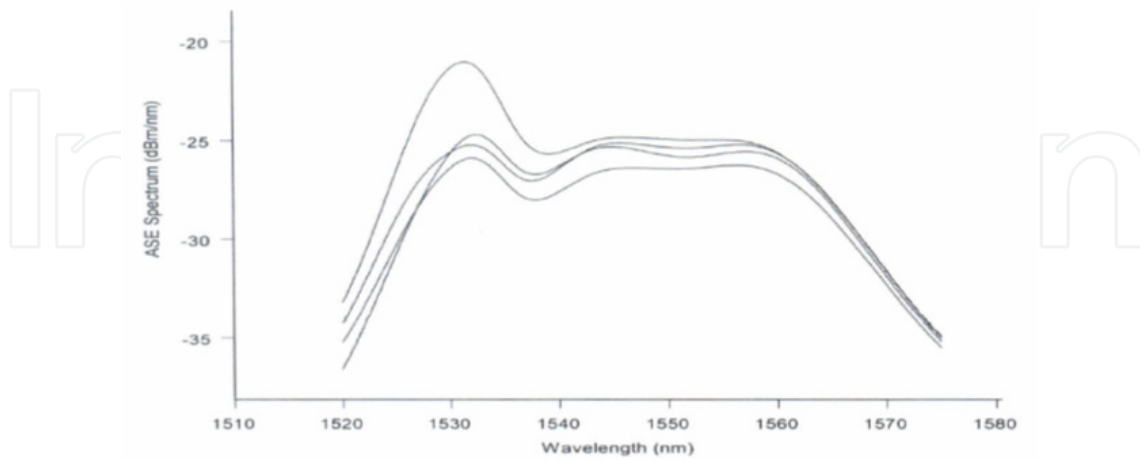
c)

Figure 13. The effect of moving the tuneable acoustic absorber on the Amplified Stimulated Emission spectrum at various gain levels: a) low gain single peak at 1560 nm b) and c) high gain two peaks at 1532 nm and 1550 nm.

Fig. 14 shows the flattened gain of ASE spectrum at various gain levels using this technique. For the lowest gain, at -30 dBm, which is achieved with a pump power of 96 mA, a broad filter is needed at 1545 nm; to obtain this; the tuneable acoustic absorber is positioned 14 cm after the AOTF device. The required resonant frequency to produce the coupling will be 990 kHz. A deeper notch is needed at 1532 nm; which is produced through the second frequency generator that is set at 993 kHz. The flattened gain is less than 0.8 dB. For gain at -25 dBm, which is achieved with a pump power of 150 mA, a filter is needed at 1556 nm; and a narrow deep notch is needed at 1532 nm; the required resonant frequency to produce the coupling respectively will be 986 kHz and 993 kHz. To obtain this, the tuneable acoustic absorber is positioned 16 cm after the AOTF device. The flattened gain is less than 0.9 dB.

Similarly for gain at -22 dBm, which is achieved with a pump power of 220 mA, a very deep filter is needed at 1532 nm and a small filter at 1545 nm. The resonant frequencies corresponding to these wavelengths are 990 kHz and 993 kHz respectively. To obtain the narrow filter, the tuneable acoustic absorber was set 17 cm after the AOTF device. And the measured flattened gain is less than 0.9 dB. Fig. 5 represents the notch filters obtained to flatten the gain of the Amplified Stimulated Emission (ASE) spectrum.
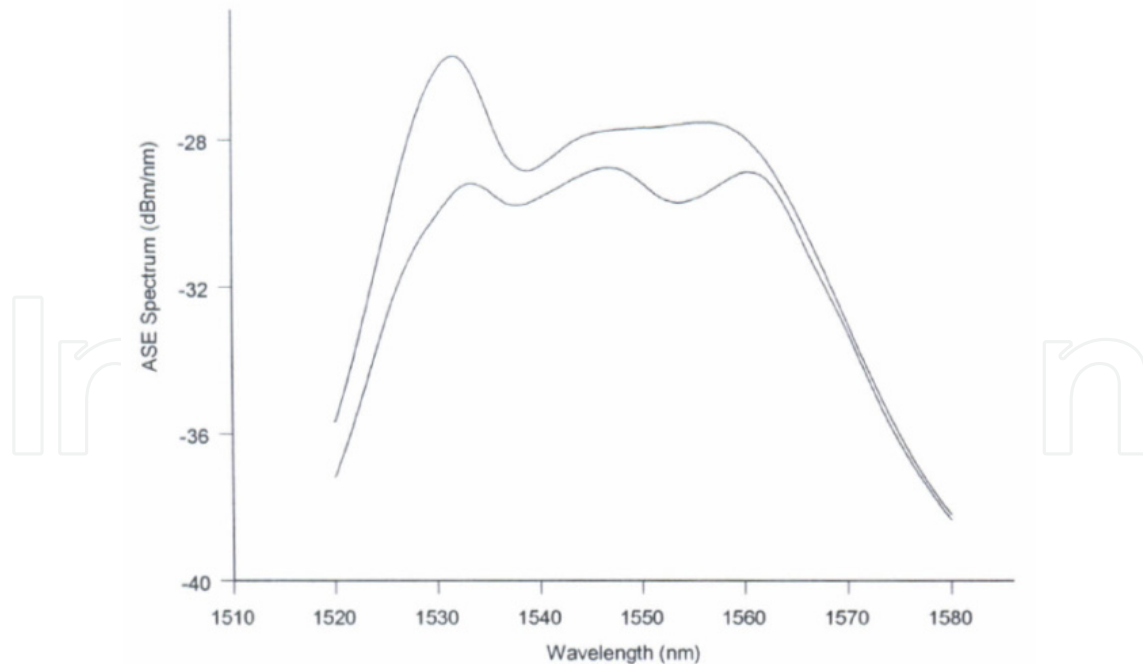
a)
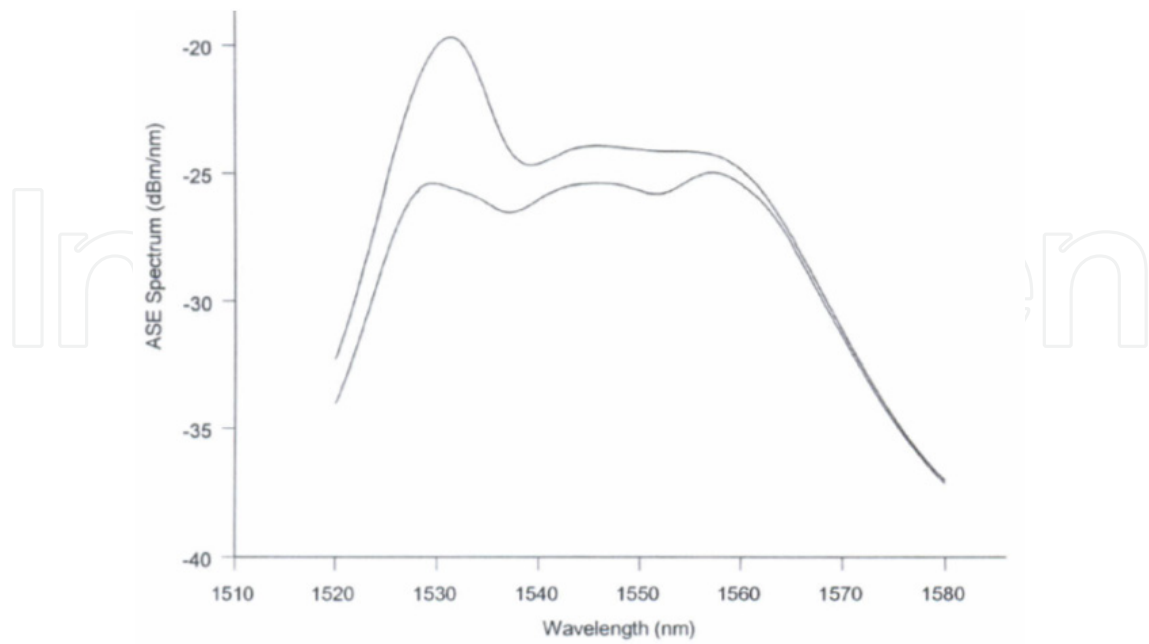
b)
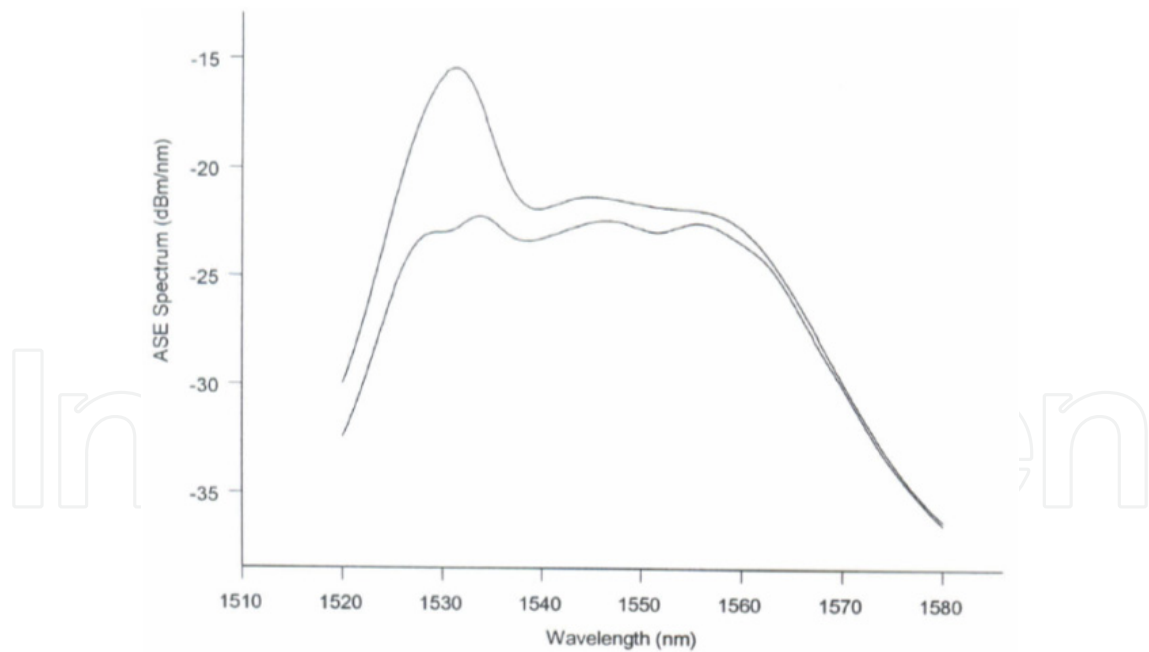
c)

Figure 14. Gain profiles of the ASE spectrum and the flattened gain at various pump powers: a) 96 mA which has a gain of -30 dBm b) 150 mA which has a gain of -25 dBm and c) 220 mA which has a gain of -22 dBm.
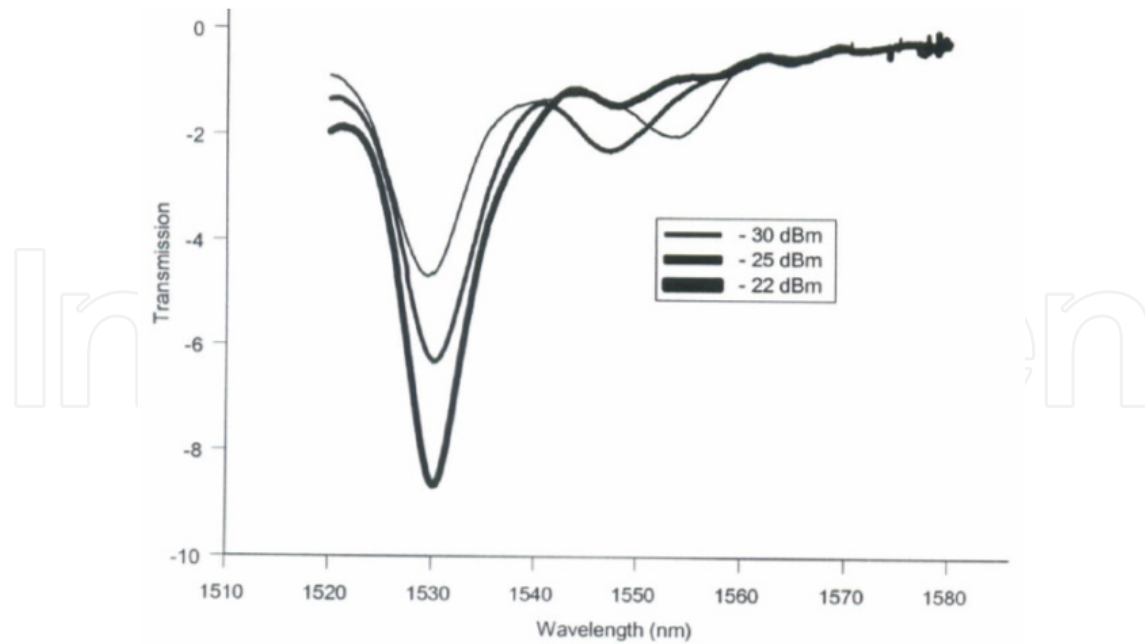
Figure 15. Corresponding filter spectrum to the flattened gain of various gain levels in Fig. 16.

7. Conclusion

The presence of acoustics inside the fiber will create a sequence of bends periodic in nature along the direction of its propagation. Core mode's energy is transferred to a cladding mode's, when it passes through the sequence of bends. The fiber jacket absorbs the coupled energy and this produces a notch filter observed using an optical spectrum analyzer.

Acoustic horn functions to transfer the acoustic wave of the transducer to the fiber. Aluminium horn is preferred over silica horn because it can be easily reproduced. Furthermore, its acoustic impedance almost matches that of silica's. To allow optimum transmission of acoustics to the fiber, the tip of the horn is made small, with its diameter matching that of silica's.

No resonance peaks were observed when the fiber is unetched First peaks are observed when the thickness of fiber is approximately 40 μ m. Overlap integral between the modes is not high in thicker fiber, meaning the transfer of acoustic wave to the fiber is not optimized. Thickness reductions in fibers are observed using a CCD camera. The characteristics of the resonance peaks can be controlled electrically using a RF generator. Voltage of the generator can be used to tune the attenuation depth of the resonance peaks. Frequency of the generator can be used to tune the peak wavelength. Frequency is inversely related to period of bends, thus higher frequencies will shift the peak to lower wavelengths. The 3-dB bandwidth of the resonance peaks can be adjusted by limiting the acoustic bend produced inside the fiber. Introducing a tunable acoustic absorber along the fiber can do this. Frequency used in all experiments was from 800 kHz to 1.1 MHz. All the coupled energy to produce the resonance peaks were to LP11 modes, mode conversion observed using a beam pro filer.

The power fed to cause resonance peaks can be reduced by reducing the thickness of the fiber to a value close to 20 μ m. Allowing light to pass through the acoustic bend region twice, as proposed in the double pass configuration, can increase the attenuation peaks. However, a frequency shift of 13 nm is observed because the light is passing through the bend in opposite directions.

As a spectral shaping tool, the attenuator is efficient as a gain flattening filter for an erbium doped amplifier. The peak of an amplified spontaneous emission at 1531 nm can be reduced to flat levels for various gains of the EDF A pump power. Insertion loss is less than 0.2 dB and polarization dependence loss is less than 0.4 dB.

Author details

Abhilash Mandloi and Vivekanand Mishra
Department of Electronics Engineering, S.V. National Institute of Technology, Surat 395007, Gujarat, India

8. References

[1] Sutharsanan Veeriah, "Design and Characterisation of All Fiber Optical Filters", Master of Science Thesis, Faculty of Engineering, Multimedia University, Malaysia, Feb 2006.

[2] Abdulhalim 1., Pannell C.N., (1993). Acoustooptic in-fiber modulator using acoustic focusing. IEEE Photonics Technology Letters, 9 (5), 999-1002

[3] Au A. A., Liu Q., Lin C.H., Lee H.P., (2004). Effects of Acoustic Reflection on the Performance of a Cladding-Etched All-Fiber Acoustooptic Variable Optical Attenuator. IEEE Photonics Technology Letters, 16 (1), 150-152

[4] Birks T.A., Russell P.SJ., Culverhouse D.O., (1992). The Acousto-Optic Effect in Single-Mode Fiber Tapers and Couplers. Journal of Lightwave Technology, 14 (11), 2519-2529

[5] Culverhouse D.O., Yun S.H., Richardson D.J., Birks T.A, Farwell S.G., Russell P.StJ., (1997). Low-loss all- fiber acousto-optic tunable filter. Optics Letters, 22 (2), 96-98

[6] Engan H.E., (2000). Acousto-Optic Coupling In Optical Fibers. IEEE Ultrasonics Symposium, 625-629

[7] Engan H.E., Kim B.Y., Blake J.N., Shaw H.J., (1988). Propagation and Optical Interaction of Guided Acoustic Waves in Two-Mode Optical Fibers. Journal of Lightwave Technology, 6 (3), 428-436

[8] Engan H.E., Ostling D., Kval Per 0., Askautrud Jan 0 .. Wideband Operation of Horns for excitation of Acoustic Modes in Optical Fibers. 10th Optical Fibre Sensors Conference, 568-571

[9] Feced R., Alegria c., Zervas M.N., (1999). Acoustooptic Attenuation Filters Based on Tapered Optical Fibers. IEEE Journal of Selected Topics in Quantum Electronics, 5 (5), 1278-1288

[10] Jung Y., Lee S.B., Lee J.W., Oh K., (2005). Bandwidth control in a hybrid fiber acoustooptic filter. Optics Letters, 30 (1), 84-86

[11] Keiser G., (1991). Optical Fiber Communications. McGraw-Hill, Inc., (2nd Edition) Kim RY, Blake J.N., Engan H.E., Shaw H.J., (1986). All-fiber acousto-optic frequency shifter. Optics Letters, 11 (6),389-391

[12] Kim H.S., Yun S.H., Kim H.K., Park N., Kim B.Y., (1998). Actively Gain-Flattened Erbium-Doped Fiber Amplifier Over 35 nrn by Using All-Fiber Acoustooptic Tunable Filters. IEEE Photonics Technology Letters, 10 (6), 790-792

[13] Kim H.S., Yun S.H., Kwang LK., Kim B.Y., (1997). All-fiber acousto-optic tunable notch filter with electronically controllable spectral profile. Optics Letters, 22 (19), 1476-1478

[14] Lee S.S., Kim H.S., Hwang LK., Yun S.H., (2003). Highly-efficient broadband acoustic transducer for all-fibre acousto-optic devices. Electronics Letters, 39 (18)

[15] Li Q., Au A.A., Lin C.H., Lyons E.R, Lee H.P., (2002). An Efficient All-Fiber Variable Optical Attenuator via Acoustooptic Mode Coupling. IEEE Photonics Technology Letters, 14 (11),1563-1565

[16] Li Q., Liu X., Lee H.P., (2002), Demonstration of Narrow-Band Acoustooptic Tunable Filters on Dispersion-Enhanced Single Mode Fibers. IEEE Photonics Technology Letters, 14 (11), 1551-1553

[17] Li Q., Liu X., Peng J., Zhou B., Lyons E.R, Lee H.P., (2002). Highly Efficient Acoustooptic Tunable Filter Based on Cladding Etched Single-Mode Fiber. IEEE Photonics Technology Letters, 14 (3), 337-339

[18] Liu Q., Chiang K.S., Rastogi V., (2003). Analysis of Corrugated Long-Period Gratings in Slab Waveguides and Their Polarization Dependence. Journal of Lightwave Technology, 21 (12),3399-3405

[19] Love J.D., Henry W.M., Stewart W.J., Black RJ., Lacroix S., Gonthier F., (1991). Tapered Single-mode fibres and devices Part 1: Adiabaticity criteria. IEE Proceedings, 138, (5), 343-354

[20] Monerie M., (1982). Propagation in Doubly Clad Single-Mode Fibers. IEEE Transactions on Microwave Theory and Techniques, MTT-30 (4), 381-388

[21] Mononobe S., Ohtsu M., (1996). Fabrication of a Pencil-Shaped Fiber Probe for Near-Field Optics by Selective Chemical Etching. Journal of Lightwave Technology, 14 (10), 2231-2235

[22] Ostling D., Engan H.E., (1995). Narrow-band acousto-optic tunable filtering in a twomode fiber. Optics Letters, 20 (11), 1247-1249

[23] Ostling D., Engan H.E., (1995). Spectral Flattening by an All-Fib er Acousto-Optic Tunable Filter. IEEE Ultrasonics Symposium, 837-840

[24] Pannell C.N., Wacogne B.F., Abdulhalim 1., (1995). In-Fib er and Fiber Compatible Acoustooptic Components. Journal of Lightwave Technology, 13 (7),1429-1434

[25] Satorius D.A., Dimmick T.E., Burdge G.L, (2002). Double-Pass Acoustooptic Tunable Bandpass Filter With Zero Frequency Shift and Reduced Polarization Sensitivity. IEEE Photonics Technology Letters, 14 (9), 1324-1326

[26] Yun S.H, Lee B.W., Kim H.K., Kim B.Y., (1999). Dynamic Erbium-Doped Fiber Amplifier Based on Active Gain Flattening with Fiber Acoustooptic Tunable Filters. IEEE Photonics Technology Letters, 11 (10), 1229-1231

[27] Yun S.H., Kim B.Y., Jeong HJ., Kim B.Y., (1996). Suppression of polarization dependence in a two-mode-fiber acousto-optic device. Optics Letters, 21 (12), 908-910

[28] Yun S.H., Kim H.S., (2004). Resonance in Fiber-Based Acoustooptic Devices Via Acoustic Radiation to Air. IEEE Photonics Technology Letters, 16 (1), 147-149